

CHAPTER 1

INTRODUCTION

Familial Hypertrophic Cardiomyopathy (FHC) is an autosomal dominant disease characterized by left ventricular hypertrophy (thickening of heart muscle), septal hypertrophy and myofibrillar disarray (disruption of normal alignment of muscle cells). FHC is the leading cause of sudden cardiac death in young athletes worldwide (1) and can affect any racial group at any age.

Mutations in one of the 9 sarcomeric genes (*MYH7*, *MYBPC3*, *TNNI3*, *TNNT2*, *TPM1*, *MYL2* and *TNNC1*) that code for sarcomeric proteins are common cause of FHC (18-21).

Contraction of cardiac muscle is responsible for blood and oxygen delivery to peripheral sites in the body from the heart. However, in the case of mutation of sarcomeric proteins the peripheral delivery efficiency of heart is lessened due to which the patient dies immediately.

Muscle fiber

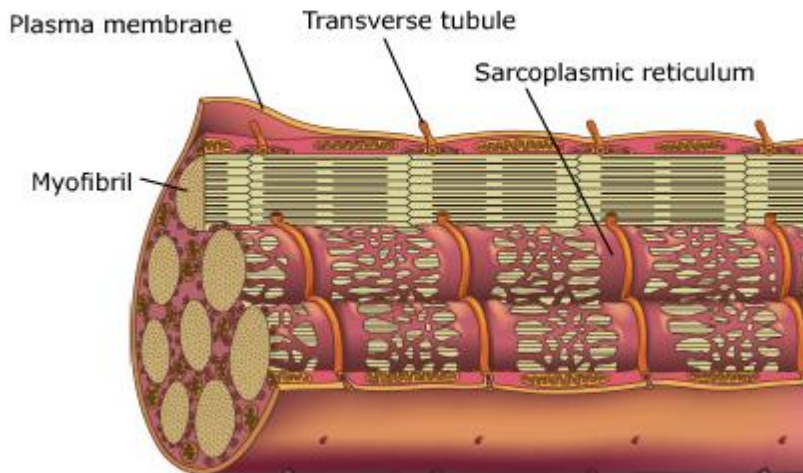


Figure1

Cardiac muscle is an involuntary striated muscle found specifically in the walls of heart (myocardium). Cardiac muscle fiber is made of myofibrils. Sub-unit of myofibrils is Sarcomere. Sarcomere is the basic unit of contraction which is made up of myofilaments like myosin (thick filament), actin (thin filament) and titin (elastic filament). The primary structural proteins in cardiac muscle contractions are actin and myosin. Cardiac muscle contraction results from periodic interaction of myosin cross-bridges with actin, during which myosin delivers force impulses to the thin filament. Basic structure and units of cardiac muscle are shown in Figure1.

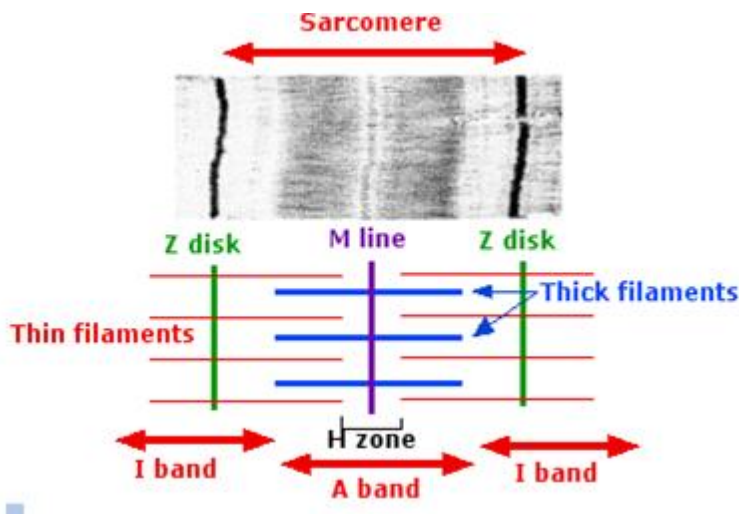


Figure2

Figure2 explains the “Sliding Mechanism of Muscle Contraction”. In this actin and myosin filaments slide over one other which results in the contraction of cardiac muscle. Myosin is molecular motor protein with enzymatic activity (ATPase). It has head, neck and tail domains:

- 1) HEAD DOMAIN- binds filamentous actin. ATP hydrolysis is used by it to generate force to move towards the barbed end (+).
- 2) NECK DOMAIN: acts as linker and transducers force generated by catalytic motor domain. Regulatory proteins like Myosin Light Chains are bound to neck domain.
- 3) TAIL DOMAIN: may regulate motor activity and functions as a mediator in interaction with cargo molecules.

Myosin has 2 clefts ATP binding cleft and Actin binding cleft, they are shown below:

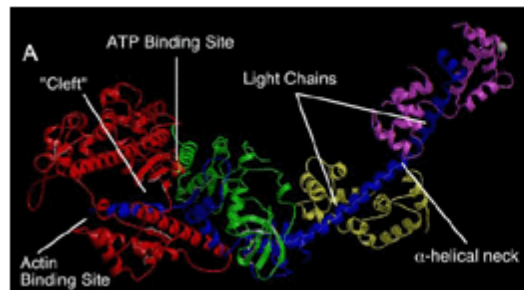


Figure3

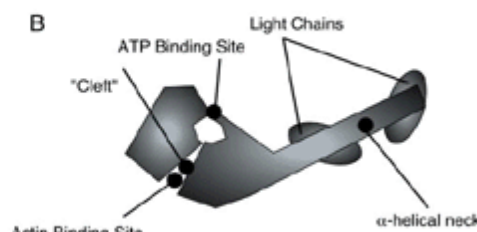


Figure4

Source- <http://www.ncbi.nlm.nih.gov/books/NBK9961/figure/A1796/?report=objectonly>

The molecular structure along with its various domains is shown in Figures 3 and 4 as Actin binding site, ATP- binding site, light chains and alpha-helical neck.

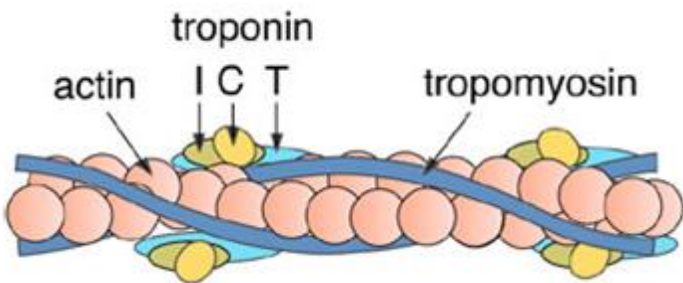
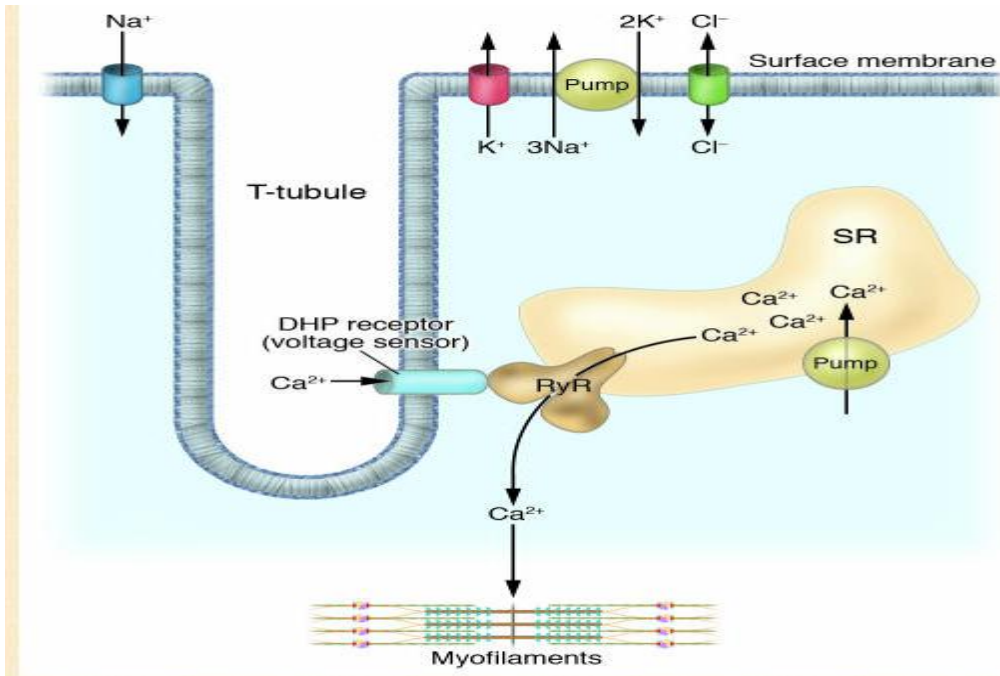


Figure5

Actin, Tropomyosin and Troponin T complex are arranged in a specific manner as shown in Figure 5. Troponin C binds to calcium ions to produce a conformational change in TnI. Troponin T binds to tropomyosin, interlocking them to form a troponin-tropomyosin complex. Troponin I bind to actin in thin myofilaments to hold the troponin-tropomyosin complex in place.

Actin is a globular protein which can exist in two forms G-Actin (monomeric) and F-Actin (filamentous). When ATP gets bound to G-Actin, it gets polymerized to form F-Actin. F-Actin has a double helical arrangement of G-Actins. Precursor for Cardiac muscle contraction is the influx of Ca⁺² ions across the T-tubules through voltage-dependent L-type Ca⁺² channels. The Ca⁺² on entering the cell bind to Ryanodine receptors on Sarcoplasmic reticulum and modulate them so that they release Ca⁺² ions from sarcoplasmic reticulum through a process known as Calcium –Induced Calcium Release (CICR). Ca⁺² released binds to Troponin –C. The conformational change in Troponin-C moves the whole Troponin complex (Troponin-I, C, T) and Tropomyosin in such a way that the Myosin binding sites are exposed on the actin filament.

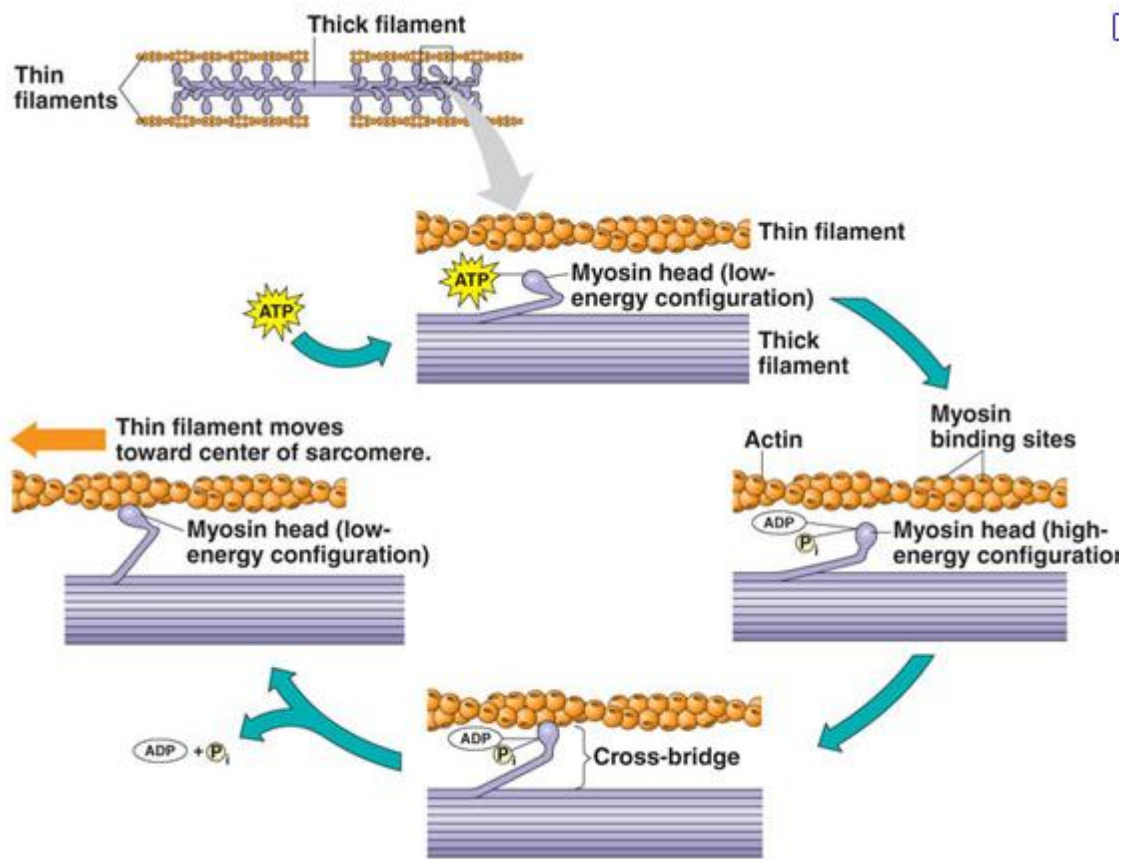


<http://people.eku.edu/ritchisong/301notes3.htm>

Figure 6

Muscle Contraction results from cyclic interactions of actin and myosin. Figure 6 shows the basic mechanism of Ca^{+2} entry and the Calcium-induced Calcium Release in cardiac cell. This CICR mechanism is responsible for the further contraction that occurs in cardiac muscle. During contraction myosin cross bridges deliver force impulses to actin. Actin slides over myosin causing contraction of muscle. Attachment of ATP to myosin head causes detachment of myosin from actin. ATP is hydrolyzed by myosin to ADP and Pi . Binding of myosin containing hydrolytic products to actin leads to Pre-Power Stroke State. The release of Pi causes force generating conformational change in bound head which forms the Post-power Stroke State in which ADP and actin are bound to myosin. This state is nearly same as rigor state. The only difference being the slight variation in the orientation of myosin. Post-power stroke state is also

called as “Weak ADP-binding state”.



Source- <http://www.google.com/imgres?imgur>
Figure 7

ADP release causes a myosin head to bind new ATP molecule, detach from actin and hydrolyze ATP (3) as shown in Figure 7 which represents the basic molecular changes that occur in Contraction. Pre and Post Power stroke state are also called closed and open states (4). From single molecule (5), structural (6) and electron microscopic studies (7) we have some evidence

for pre and post power stroke states. Details of power stroke are obtained by following the motion of mesoscopic assembly of molecules (affected by fluctuations around average) (8). For this 3-4 myosin molecules are observed in a small confocal volume, whose neck region are tagged with LC1.

The goal of our investigation is to quantify the distribution of orientations of myosin in Troponin T mutated heart muscles samples (F110I, R278C and I79N) and compare them with wild type ones.

Troponin-T is one of the 3 regulatory proteins of Troponin complex. It binds to tropomyosin, interlocks them tightly and forms troponin-tropomyosin complex. It plays important role in contraction of striated muscle, provides structural stability to troponin complex and participates in Ca⁺² –dependent regulation of contraction (12-14). TnT association with FHC was found in 1994 (15).

The F110I mutation occurs in a conserved region of TnT that interacts with actin and Tropomyosin and R278C mutation is located in region of positively charged residues reported to interact with TnT, TnI and Troponin C (16-17). Recent findings have shown that these TnT mutations have been responsible for functional defects in contractile apparatus leading to FHC. The R278C mutation has been found to have a lower disease penetration than F110I mutation.

Here we have carried out measurements using single molecule detection (SMD). The rationale for SMD measurements is that humans are heterozygous for FHC i.e., hypertrophic myocardium contains a mixture of wild-type (WT) and mutated protein. Previous studies have shown that Tg-TnT mice expresses 50% of mutant protein in heart (22-23). So it is

likely that only 50% of myosins interact with actin that carries the mutated TnT. This may not lead to a significant change in the Global properties of muscle, even though some changes in isometric tension, ATPase and Ca⁺² sensitivity have been reported (22-23).

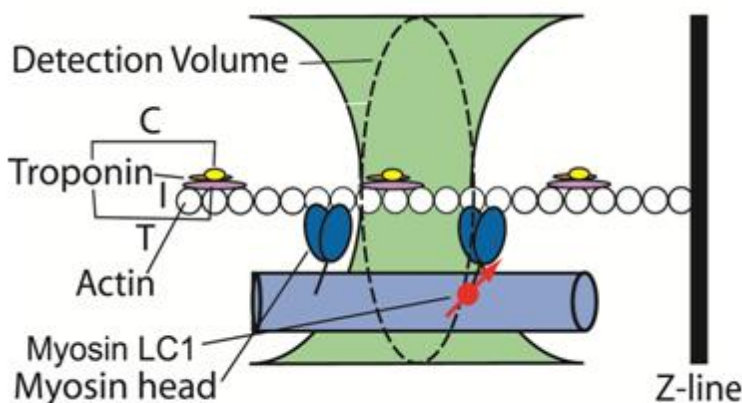


Figure 7

Rationale behind the method used to collect the data is illustrated by Fig8. Myosin light chain1 (LC1) is lightly labeled with rhodamine and exchanged with native LC1 of a myofibril (MF). A small volume within the A-band is illuminated by a laser beam focused to the diffraction limit (green). The fluorescence is observed by a microscope through a small pinhole (confocal detection) so the detector sees only the volume indicated by a dashed line. It is an ellipsoid of revolution whose volume is approximately $1 \mu\text{m}^3$. Because myosin is labeled very sparsely (only one of approximately 60,000 myosin molecules carry fluorescent LC1), this detection volume (DV) contains only ~5 fluorescent molecules (see the section “Number of observed molecules” in Results). Myosin cross-bridges in contracting muscle undergo periodic changes of orientation

due to power stroke and to association-dissociation from actin leading to fluctuations in polarized fluorescence of rhodamine. The distribution of orientations reflects on relative occupancy of different enzymatic states. Myosin cross-bridges in rigor muscle do not rotate, but the distribution of orientations reflects on how well they are organized. Fluctuations are recorded by measuring parallel (\parallel) and perpendicular (\perp) components of fluorescent light. The normalized ratio of the difference between these components is called Polarized Fluorescence (PF) and is a sensitive indicator of the orientation of the transition dipole of the fluorophore [2-4, 9-13]. We characterize fluctuations by velocity plots (the rate that a given polarization changes), by Full-Width Half Maximum(FWHM)and by skewness and kurtosis of histograms. A histogram is a diagram showing the size of fluctuation on x-axis and the number of times that a given fluctuation occurs on y-axis. A positive skewness means that the tail of the curve points towards positive values of the histogram. A positive kurtosis is expressed by long tails and higher peaks compared to the Gaussian curves. A negative skewness means that the tail of the curve points towards negative values of the histogram. A negative kurtosis means that the tails are smaller than those of Gaussian curves.

We report that the distribution of orientations in rigor WT and MUT myofibrils were significantly different. There was large difference in the velocity plots, FWHM and the values of both skewness and kurtosis. These findings suggest that the hypertrophic phenotype associated with the TnT mutations can be characterized by a significant increase in disorder of rigor cross-bridges.

CHAPTER 2

MATERIALS AND METHODS

Chemicals and solutions. Tetramethylrhodamine-5-iodoacetamide dihydroiodide (5-TMRIA) (single isomer) was purchased from Molecular Probes (Eugene, OR, Cat. No. T-6006). All other chemicals were from Sigma-Aldrich (St Louis, MO). The composition of solutions was as in [14]. Briefly: the Ca-rigor solution contained 50 mM KCl, 0.1 mM CaCl₂, 10 mM Tris pH 7.5, 1 mM DTT. Contracting solution had the same composition plus 5 mM ATP. Mg²⁺-rigor solution had the same composition except that 2 mM MgCl₂ replaced Ca²⁺. EDTA-rigor had the same composition except that it did not contain either Mg²⁺ or Ca²⁺ and contained in addition 5 mM EDTA.

FHC-TnT mutations in mice. The degree of the human TnT expression in the Tg mouse hearts were 71%, 52%, 45% and 50% for L3-WT, L8-I79N, L1-F110I and L5-R278C mutations, respectively [5, 6]. The mice were euthanized according to the approved protocol by the animal care and use committee (IACUC) of the Miller School of Medicine University of Miami. After euthanasia, the hearts were immediately frozen and stored at - 80°C until needed. The Tg hearts used in this study were ~ 3 to 7 months-old. The frozen hearts were thawed and then briefly rinsed (no more than 30 s) with ice-cold 0.9% NaCl. Muscle strips from left and right ventricles and papillary muscles were dissected at 4 °C in a cold room in ice-cold pCa 8 solution (10-8 M [Ca²⁺], 1 mM [Mg²⁺], 7 mM EGTA, 2.5 mM [MgATP²⁺], 20 mM MOPS, pH 7.0, 15 mM creatine phosphate, ionic strength = 150 mM adjusted with potassium propionate) containing 30

mM BDM and 15% glycerol [14] . After dissection, muscle strips were transferred to pCa 8 solution mixed with 50% glycerol and incubated for 1 h on ice. Then the muscle strips were transferred to fresh pCa 8 solution mixed with 50% glycerol and containing 1% Triton X-100 for 24 h at 4 °C. Muscle strips were finally transferred to a fresh batch of pCa 8 solution mixed 1:1 with glycerol and kept at – 20 °C until used for the preparation of myofibrils.

LC1 Expression. Light Chain 1 expression was done as described previously [15]: Briefly, pQE60 vector containing recombinant LC1 (single cysteine residue) was donated by Dr. Lowey (University of Vermont). The DNA plasmid was transformed into E.coli M15 competent cells and recombinant clones were selected by ampicillin resistance. The clones containing LC1-cDNA insert were confirmed by DNA sequencing (Iowa State University of Science and Technology). LC1 protein was over expressed in Luria broth containing 100 µg/ml of ampicillin by inducing with IPTG. His-tagged LC1 protein was affinity purified on Ni-NTA column. The imidazole eluted fractions were run on SDS-PAGE followed by Western analysis with Anti-LCN1 antibody (Abcam, CA). Fractions containing LC1 were pooled together and dialyzed against buffer containing 50 mM KCl and 10 mM phosphate buffer (pH 7.0). Purified protein showed a single band migrating on SDS-PAGE at ~25-kDa [15].

Preparation of myofibrils. Left or right ventricular muscle from Tg mice (mutated or WT) was washed with an ice-cold EDTA-rigor solution for 0.5 hr followed by an extensive wash with Mg²⁺-rigor solution to prevent contraction while ATP was being removed. This was followed with wash with Ca²⁺-rigor solution and homogenization using a Heidolph Silent Crusher S homogenizer for 20 s (with a break to cool after 10 s). We noted that foam formed when a muscle was homogenized in EDTA-rigor solution.

LC1 labeling: LC1 was dialyzed against buffer A [50mM KCL and 10mM phosphate buffer (pH 7.0)] and fluorescently labeled by incubating with 5 molar excess of 5-TMRIA for 6 h in buffer A on ice. Unbound dye was eliminated by passing the solution through Sephadex G50 columns. The concentrations of LC1 protein and bound 5-TMRIA were determined to estimate the degree of labeling. Protein concentration was determined by Bradford assay and 5-TMRIA CA) spectrometer. The concentration of both the protein and 5-TMRIA dye was found to be the same (10 μM), indicating that the degree of labeling was 100%.

LC1 exchange into myofibrils: Rhodamine labeled LC1 (R-LC1) was incubated with 1 mg/ml of freshly prepared myofibrils in exchange solution [15mM KCl, 5mM EDTA, 5mM DTT, 10mM KH₂PO₄, 5mM ATP, 1mM TFP, and 10mM imidazole pH 7] [16] for 5 minutes at 30°C. Concentration of R-LC1 was 3 nM unless otherwise specified.

Cross-linking. Polarized intensities during contraction are impossible to record reliably unless muscle shortening is effectively abolished. In our experiments shortening was abolished by cross-linking with water-soluble cross-linker 1-ethyl-3-[3-(dimethylamino)propyl]carbodiimide (EDC)[17, 18]. Briefly: myofibrils (1 mg/ml) were

incubated with 20 mM EDC for 20 min at room temperature. The reaction was stopped by adding 20 mM DTT. The lack of shortening was checked by imaging myofibrils by differential contrast microscope, and by fluorescence microscope after labeling myofibrils with 10 nM rhodamine-phalloidin [19]. Cross-linking had no effect on probability distribution measurements [15].

Sample preparation. In contrast to skeletal myofibrils, cardiac myofibrils attached weakly to the glass and were easily displaced by washing. In order to attach them strongly the coverslips were cleaned with 100% ethanol and spin coated with Poly-L-lysine solution (Sigma-Aldrich 0.1%) at 3,000 rpm for 120s using a spincoater P6700 (Specialty Coating Systems, Indianapolis, Indiana).

Rigor force measurements in skinned cardiac papillary muscle fibers. The frozen hearts were thawed and the papillary muscle fibers were isolated. The muscle fibers were then skinned according to Baudenbacher et.al [20]. Briefly, small bundles of fibers were isolated and placed in a pCa 8.0 relaxing solution (10–8 M [Ca²⁺]free, 1 mM [Mg²⁺]free, 7 mM EGTA, 2.5 mM MgATP₂-, 20 mM MOPS (pH 7.0), 20 mM creatine phosphate, and 15 units/ml creatine phosphokinase, I = 150 mM) containing 1% triton X-100 and 50% glycerol at 4°C for approximately 4-6 hours. Fibers were then transferred to the same solution without triton X-100 and stored at -20°C for up to four days. Mouse muscle fiber bundles with a diameter varying between 65 – 139 mm and ~ 1.3 mm of length were attached to tweezer clips connected to a force transducer. To ensure complete membrane removal and complete access to the

myofilament, the fibers were treated with pCa 8.0 containing 1% Triton X-100 for 30 min before the beginning of the experiment. To remove the excess Triton X-100 from the fibers, extensive washing was carried out with pCa 8.0 and then the functional parameters were evaluated. To determine the rigor force under relaxing conditions, the fiber was first extensively rinsed in a pCa 8.0 solution without ATP and then allowed to reach the maximal rigor force in the same solution. However, to determine the rigor force under activating conditions, the fiber was first allowed to contract in pCa 4.0 (in the presence of ATP) and then extensively rinsed in a pCa 4.0 solution without ATP. The fiber was then allowed to reach a plateau and this was considered as the maximal rigor force under activating conditions.

Probability distribution measurements. Alba-FCS (ISS Co, Urbana, IL) confocal system coupled to an Olympus IX 71 microscope was used. The data were collected every 10 μ s and was smoothed by binning 1000 points together. The instrument was calibrated and optimized every day with 50 nM solution of rhodamine G. Optimization was carried out until the G-factor (ratio of the orthogonal components) was 1. The excitation was by a 532 nm CW laser. A polarizer was inserted before the entrance to the microscope to ensure that the exciting light was strictly linearly polarized and vertical on the microscope stage. The laser power was attenuated so as not to illuminate a sample with more than 100 μ W. The confocal aperture was 50 μ m. The emitted light was split 50/50 by a prism and each component was detected by a separate Avalanche PhotoDiode (APD). The parallel (\parallel) and perpendicular (\perp) (with respect to the laboratory frame of reference) analyzers were inserted before detectors with the result that APD's of channels 1 and 2 measured the polarized intensities oriented \perp and \parallel to the myofibrillar axis, respectively.

MFs were always placed with the axis pointing vertically on the microscope stage, i.e. their long axis was always parallel to the direction of polarization. Therefore according to the conventional notation [12] we measure parallel polarization of fluorescence (PF_{\parallel} , the subscript denoting direction of excitation polarization with respect to myofibril axis).

Time resolved anisotropy. To test whether rhodamine was rigidly immobilized on the surface of LC1 so that the orientation of the transition dipole of the fluorophore reflects the orientation of the neck of myosin head, we measured the decay of anisotropy of R-LC1 exchanged into skeletal myofibrils. Fluorescence anisotropy was measured by the time-domain technique using FluoTime 200 fluorometer (PicoQuant, Inc.). The excitation was by a 532 -nm laser pulsed diode. The emission was observed through a monochromator at 590 nm with a supporting 590-nm long wave pass filter. The FWHM of pulse response function was 70 ps. Time resolution was better than 10 ps. The intensity decays were analyzed in terms of a multi-exponential model using FluoFit software (PicoQuant, Inc.). All experiments were performed at ~23°C. The decay of anisotropy [defined as $r=(I_{\parallel}-I_{\perp})/(I_{\parallel}+2I_{\perp})$] of free TMRIA was best fitted by a double exponential curve $r(t)=R_{\infty}+a \cdot \exp(-t/\theta_1) + b \cdot \exp(-t/\theta_2)$ where $R_{\infty}=0.05$ was the value of anisotropy at infinite time and $\theta_1=0.3$ and $\theta_2=608.7$ ns were the rotational correlation times. The fast decay dominated the signal (93.1%) - the slow correlation time comprised only 6.9 % of the decay, probably contributed by aggregates of rhodamine. The decay of R-LC1 in skeletal myofibrils was best fitted by the same double exponential function, but R_{∞} was 0.33, θ_1 was 67.7 and θ_2 was 0.9 ns. The slow correlation time comprised 82.1% and the fast correlation time 17.9

% of the decay. The short and long correlation times were most likely due to the rotation of rhodamine moiety on LC1 and to rotation of bound LC1, respectively. The maximum value of anisotropy was 0.384. The high value of initial anisotropy indicates that the absorption and emission dipoles of rhodamine are nearly parallel. Thus the mobile fraction was contributed by the minority of fluorophores and we conclude that LC1 labeling is appropriate for measuring polarization of muscle.

Statistical analysis It was carried out using Systat (SigmaPlot 11.02 and Origin software (Origin v. 8.5, Northampton, MA). Goodness of fit was assessed by reduced χ^2 . Non-linear curve fitting was performed in Origin, which uses the Levenberg-Marquardt algorithm to perform chi-square minimization. The custom software of "velocity" plots (available on request) was written with Labview 2010. Velocities were calculated by taking the difference of consecutive position data points and dividing it by the difference of the time stamps associated with each data point. The plot is the array of velocity data points versus the array of polarization points on an x-y plot. The front panel of Labview program is comprised of a view graph, buttons for initializing the process, storing the data as an excel file, and exporting a graph of the data as a .jpg file. The program was compiled using Labview's compiler into a stand alone executable.

CHAPTER 3

RESULTS

Global Measurements. We first show that by measuring global parameter (rigor tension) it is impossible to distinguish between NTg and Tg-mutated heart preparations.

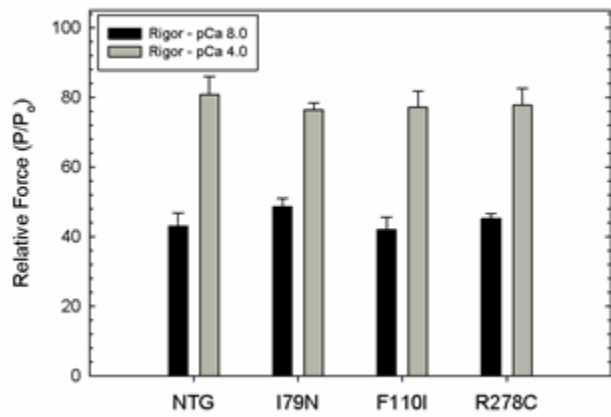


Fig. 9

Fig. 9 shows that the

rigor tension developed by NTg muscle was not different from average rigor force developed by mutated muscle either in rigor-pCa 8.0 or rigor-pCa 4.0. Non transgenic (NTg) MF were used as a control for the cardiac skinned papillary muscle fibers, instead of Tg-WT. The difference between the two is that Tg-WT mice carry the human cardiac TnT in the mouse cardiac myofilament background. Previous studies have shown that papillary muscles of both mice (Tg-WT and NTg) develop similar maximal force and have similar Ca^{2+} sensitivity [5, 6].

Mesoscopic measurements. To examine few cross-bridges, rather than to observe a global parameter of muscle, measurements were done on myofibrils, as illustrated in **Fig. 10. A and B** show typical orthogonal fluorescence intensity images of a single Tg-F110I myofibril from the

right ventricle of a mouse in rigor.

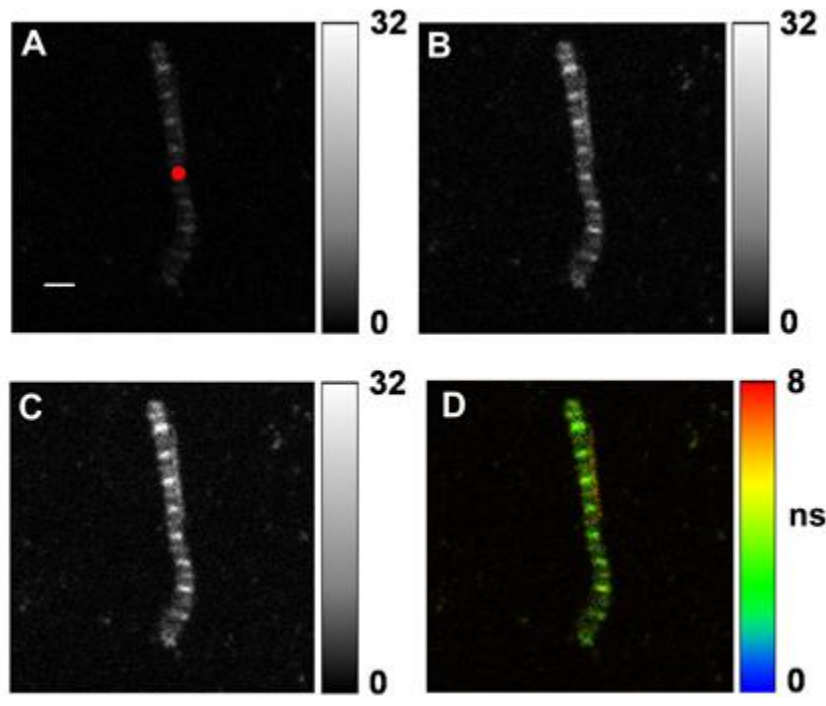


Fig. 10.

The image is fainter when the emission polarization is perpendicular to the direction of polarization of exciting light than when it is parallel indicating that the absorption/emission dipole of the dye is largely perpendicular to the axis of a myofibril. D is fluorescence lifetime image. In contrast to skeletal muscle, where nebulin prevents phalloidin from labeling all-but the pointed ends of actin filaments [21, 22], in the nebulin-free heart muscle the entire I-bands are labeled. The dark areas do not contain actin (H-bands). The red circle is a 2D projection of the confocal aperture on the image plane. Its diameter is equal to the diameter of the confocal aperture ($50 \mu\text{m}$) divided by the magnification of the objective (40x). The data is collected from the detection volume(DV)of which red circle in A is projection.

Number of observed molecules. To assure that only a small number is observed, native LC1 of myosin was exchanged with a small (3 nM) concentration of labeled LC1. To estimate the number of molecules contributing to the observed fluorescence, we measured signal intensity at decreasing (8.5-1.7 nM) concentrations of the dye. The Detection Volume (DV) at the focus of the confocal microscope is an ellipsoid of revolution whose waist (1.2 μm) is equal to the diameter of the confocal pinhole ($2\omega_0=50 \mu\text{m}$) divided by the magnification of the objective (40x). The ellipsoid is assumed to have a waist ω_0 and height, z_0 , equal to the thickness (1 μm) of a typical myofibril. Therefore $DV=4/3\pi\omega_0^2z_0$ is $\sim 1 \mu\text{m}^3$. This is approximately equal to the volume of a typical half-sarcomere. Knowing the DV and concentration we calculated the number of molecules in the DV. The concentration of 1.7 nM TMRIA corresponds to a single fluorophore. Extrapolation of the signal intensity-concentration curve to 1.7 nM yields number of photons per one fluorophore ≈ 750 counts/s. It is now possible to estimate the number of molecules contributing to the actual signal. **Fig.11** shows the intensities of perpendicular (black, ch1) and parallel (red, ch2) channels of rigor (top panel) and contracting (bottom panel) obtained from a typical myofibril. The average intensities were 14 and 12 counts/10 ms for rigor and 50 and 62 counts/10 ms for contraction, respectively (note that **Fig. 11** is a bar plot). The average was 3500 counts/s. This corresponds to ~ 5 myosin molecules.

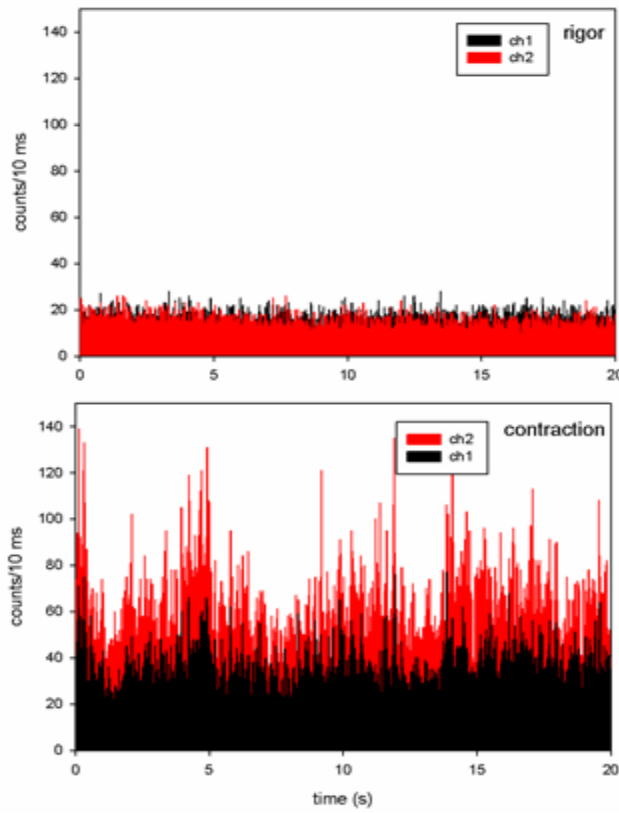


Fig.11

A direct confirmation of this estimation was obtained by calculating the autocorrelation function of fluctuations. In this method the number of observed molecules is measured directly by obtaining the autocorrelation function (ACF) of fluctuations of the fluorescence. The value of the autocorrelation function at delay time 0 [$G(0)$] is equal to the inverse of the number of molecules N contributing to the signal, $N=1/G(0)$ [23, 24]. **Fig.12** shows the typical correlation function of contracting I79N mutated myofibrils. $1/G(0)=0.2$ indicating that the number of molecules contributing to fluctuations is 5.

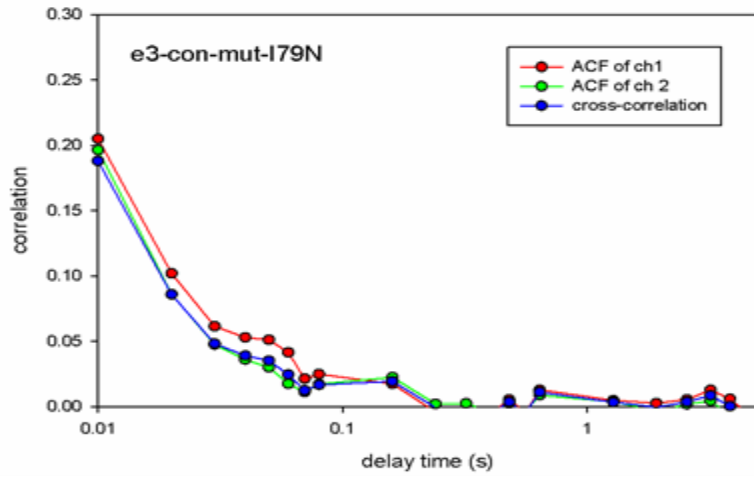


Fig.12.

Dispersion of rigor orientations. The rigor distribution of mutated and WT myofibrils differ in width and in the position of the center. Good qualitative illustrations of the differences in the width are "velocity" plots where the "angular velocity" is plotted against PF. The "angular velocity" is defined as the difference of PF at consecutive times divided by 10 ms (hence "angular", because PF is related to the angle of the transition dipole of the dye). Of course it is not actual velocity, which is 0 in rigor. It merely has units of velocity and is introduced here to create 2D plots of PF. The plots contain the information contained in all 25 experiments done for each mutation. One experiment contains 2000 measurements of PF, i.e. a velocity plot contains 50,000 points.

The differences between WT and MUT of rigor myofibrils for each mutation are shown by Figure 13.

It is clear that the distribution of polarizations is narrower in WT myofibrils (green) than in MUT myofibrils (red).

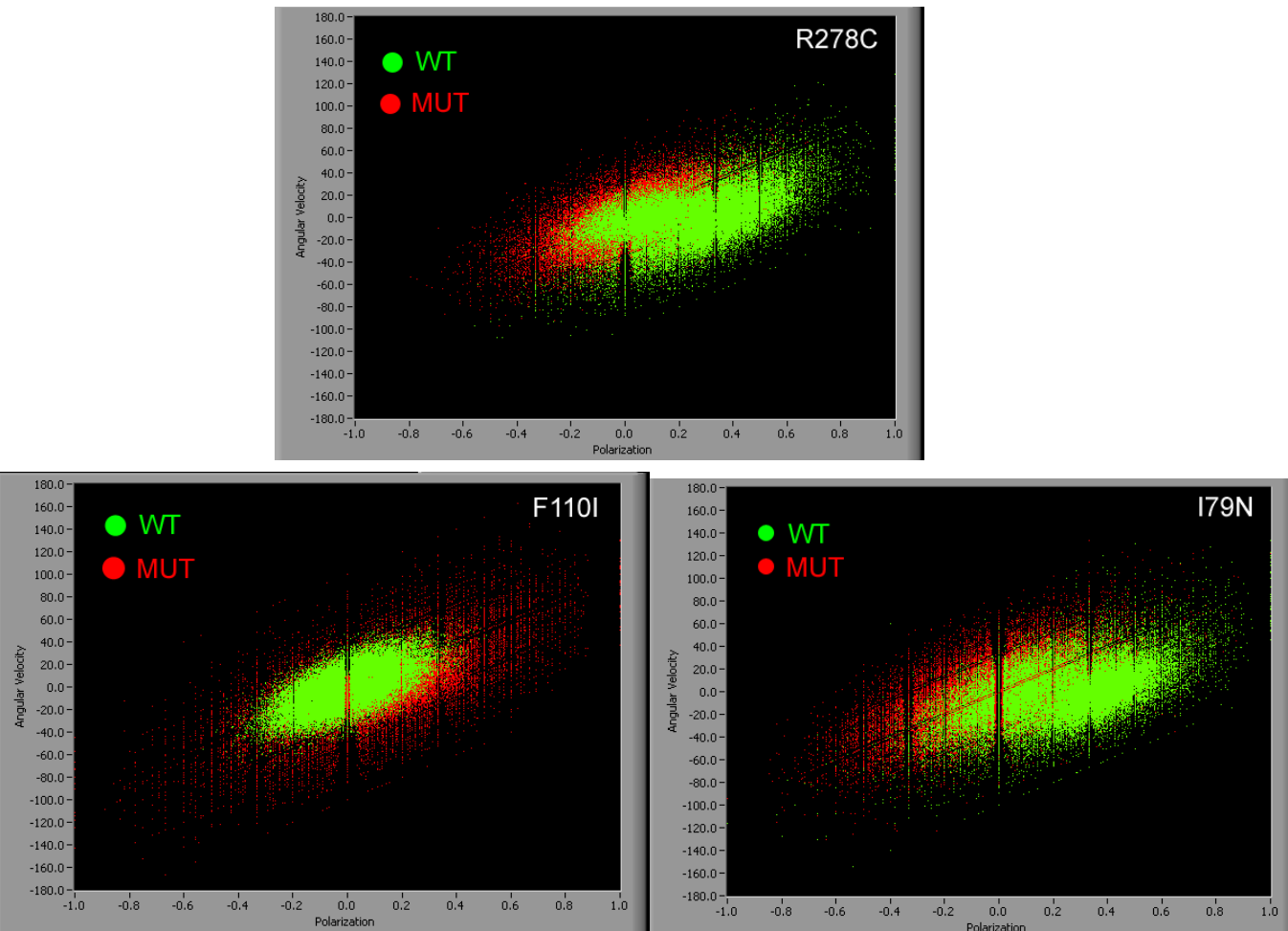


Figure 13

The differences in the center of rigor WT and MUT distributions are best illustrated in "energy" plots, where the square of angular velocity (proportional to "energy") is plotted against PF (Fig. 14). As before, the plots contain the information contained in all 25 experiments done for each

mutation. One experiment contains 2000 measurements of PF, i.e. an energy plot contains 50,000 points.

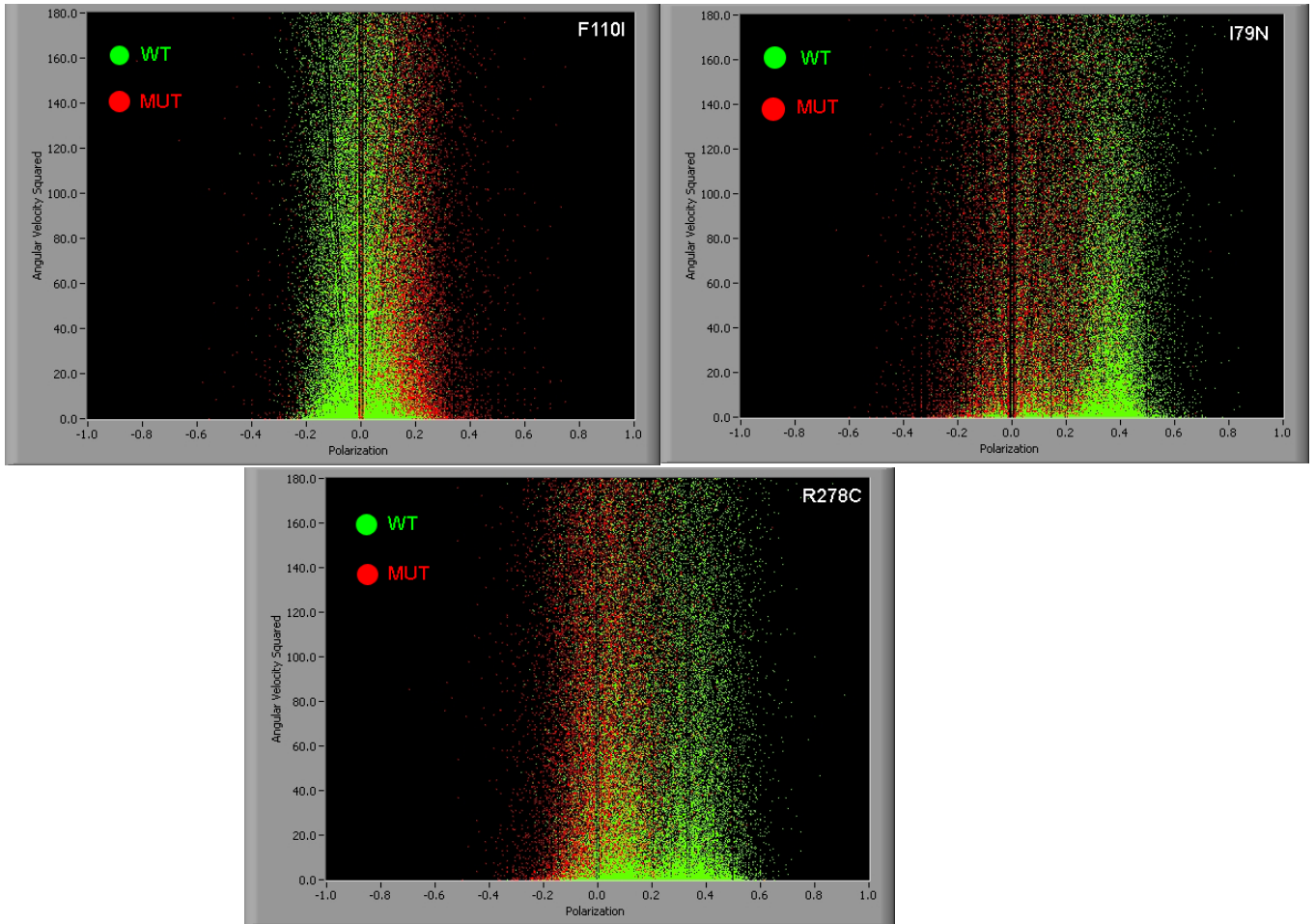


Figure 14.

The meridional lines in **Figs. 13** and **14** arise because polarization, defined as normalized number of \parallel polarized photons minus number of \perp polarized photons, can assume only discrete values. Similarly, the equatorial lines arise because velocity is defined as $\Delta\text{PF}/\Delta t$. For each

mutation 25 experiments were done.

A histogram is a plot of the number of events of a given polarization value occurring during 20 s experiment [25]. Myofibrils were prepared at the same time from the same muscle. The histograms were fitted with a Gaussian curve $y=a \exp[-0.5(x-x_0/b)^2]$ and skewness and kurtosis were computed by SigmaPlot v. 11 program. The key finding is that the histograms of mutated myofibrils in rigor were more disperse than histograms of rigor-WT myofibrils. Figures 15-17 show the histograms for each type of mutation in rigor state. The quantified difference is shown in Table 1 which lists the center and FWHM for each mutation.

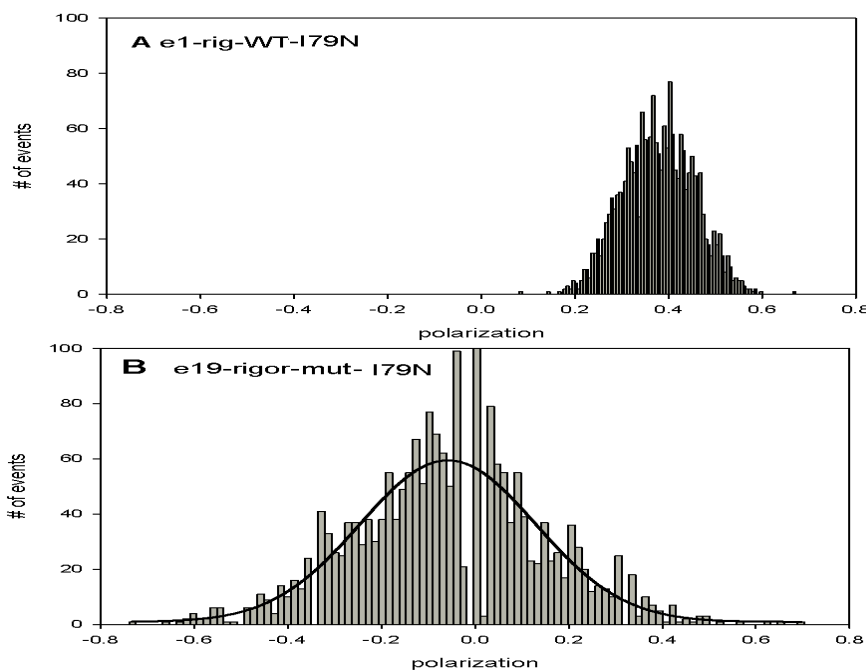
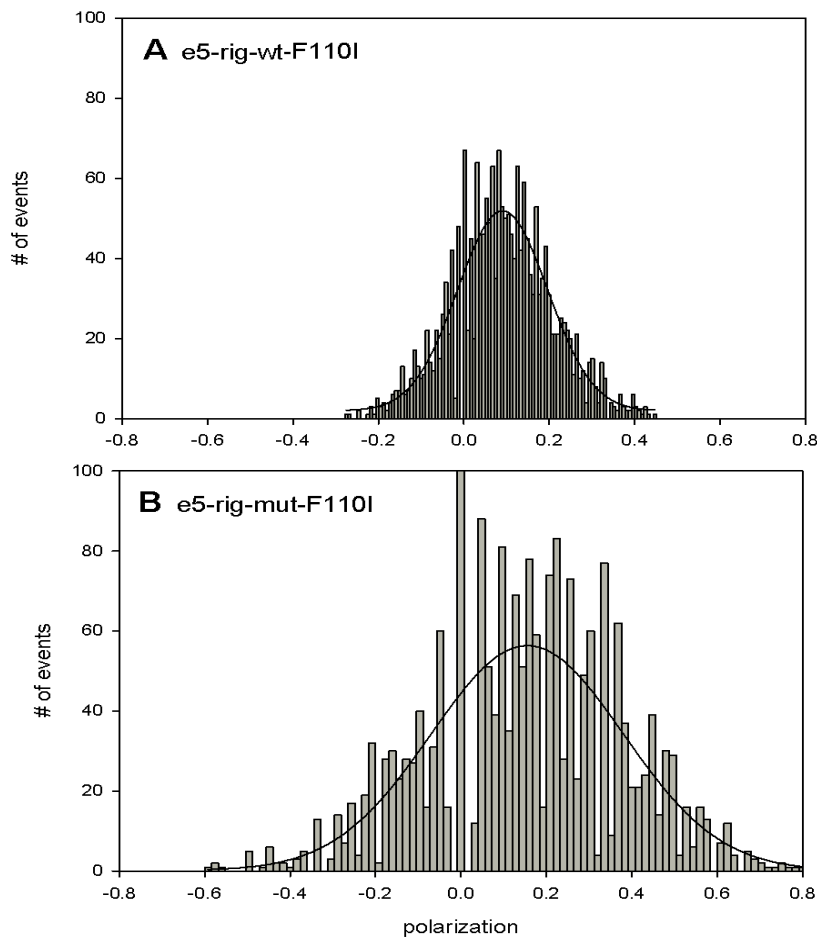


Figure 15

Figure16



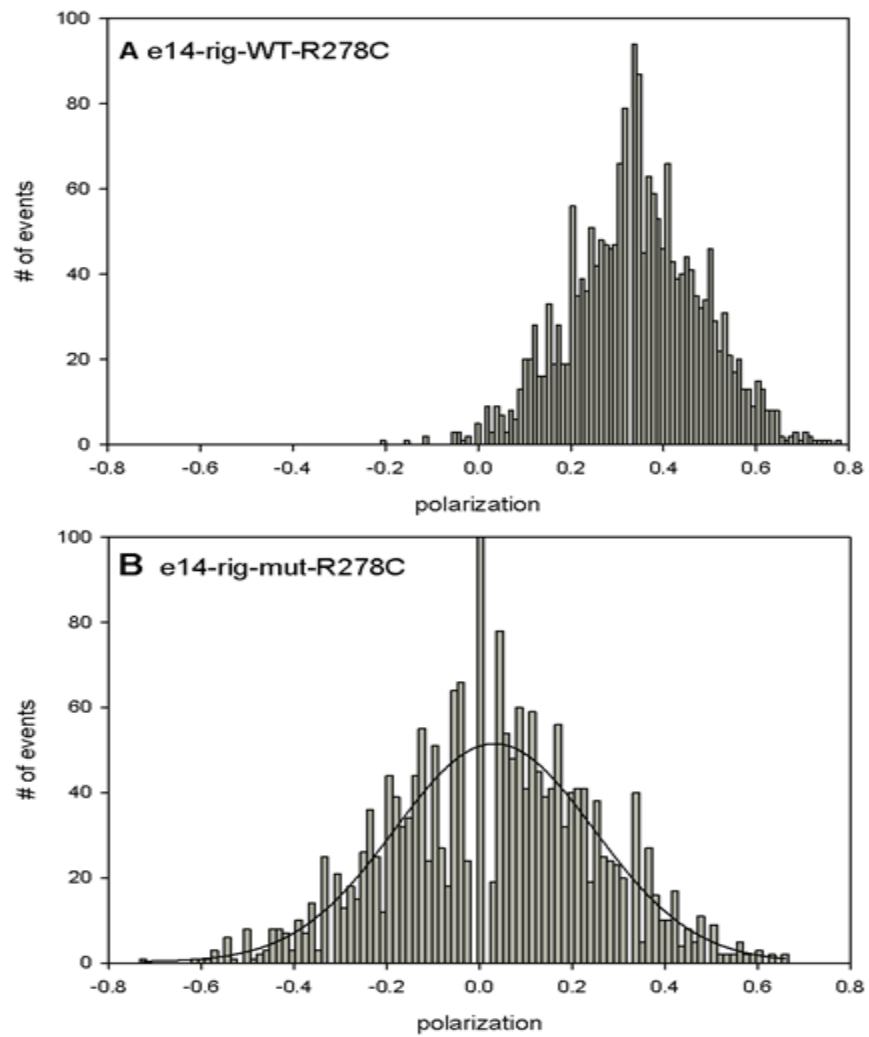


Figure 17

Sample	FWHM±SD	Peak±SD
I79N-WT	0.29±0.10	0.26±0.14
I79N-MUT	0.32±0.09	0.04±0.14
F110I-WT	0.22±0.01	0.00±0.04
F110I-MUT	0.34±0.18	0.10±0.08
R278C-WT	0.20±0.07	0.26±0.12
R278C-MUT	0.28±0.06	0.04±0.09

Table 1

Since FHC mutations are expressed at ~50% level it should be possible to subdivide data into two sets, clustering around different polarizations. This was indeed the case as shown in figure 18 where the angular velocity measurements of mutated and wild-type were plot: the data from mutated myofibrils could always be divided into two approximately equal populations, clustering around small and large polarizations. This presumably corresponds to myofibrils carrying a mutation, and myofibrils which were classified as mutated but that carried no mutation.

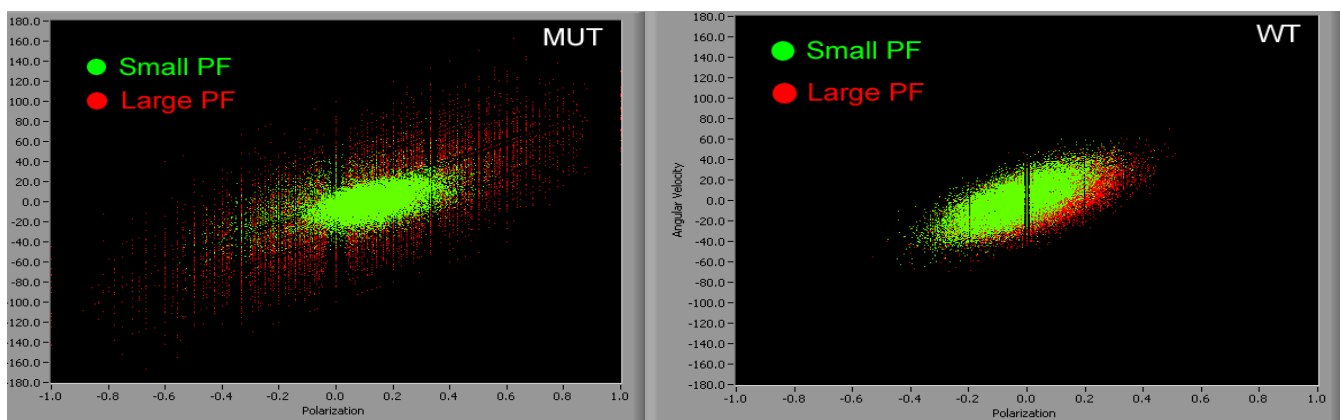


Fig. 18

Left panel in Figure 18 shows the distribution of experimental points in 50,000 measurements on myofibrils carrying F110I mutation. The values of polarizations clearly are clustered around small (green) and large (red) values of PF. The dispersion of rigor histograms was quantified by the value of Full Width at Half Maximum of a single Gaussian fit.

Table2.

Sample	FWHM
Average for WT	0.25±0.05
F110I-MUT-lowPF	0.14±0.02
F110I-MUT-highPF	0.48±0.09
R278-MUT-lowPF	0.29±0.03
R278C-MUT-highPF	0.31±0.06
I79N-MUT-lowPF	0.22±0.03
I79N-MUT-highPF	0.39±0.06

Table 2 shows that PF clusters around two distinct values. The differences between FWHM of histograms of WT and the value of high PF of MUT rigor myofibrils were statistically highly significant. This suggests that high PF of MUT myofibrils represents mutated fraction, and low PF of MUT myofibrils represents non-mutated fraction.

No clustering occurs in experiments on WT myofibrils (**Fig. 18**, Right panel). Similar results were obtained for other mutations.

Skewness and Kurtosis. To characterize data further, we computed skewness and kurtosis of histograms. A positive skewness means that the tail of the curve points towards positive values of the histogram [28]. A negative skewness means that the tail of the curve points towards the negative values of the histogram. A positive kurtosis is expressed by

long tails and lower peaks compared to the Gaussian curves and a negative kurtosis means that the tails are smaller and the peaks are taller than those of Gaussian curves. The values for F110I, R278C and I79N mutations are summarized in **Tables 3-5**. The differences in skewness between all the heart preparations, whether mutated or not, were not statistically significant. However, the differences in kurtosis between all the TnT mutations in rigor and the values for all other conditions are significant.

Table 3. Mean and Standard Deviation of Skewness and Kurtosis of 25 heart muscles expressing I79N mutation.

Sample	Skewness±SD	Kurtosis±SD	Peak±SD
I79N-WT-rigor	1.24±0.55	1.48±2.95	0.26±0.14
I79N-MUT-rigor	1.44±0.58	2.71±3.40	0.04±0.14
I79N-WT-con	1.06±0.31	0.25±1.22	0.28±0.03
I79N-MUT-con	0.85±0.21	-0.49±0.69	0.21±0.08

Table 4. Mean and Standard Deviation of Skewness and Kurtosis of 25 heart muscles expressing F110I LV mutation.

Sample	Skewness±SD	Kurtosis±SD	Peak±SD
F110I-WT-rigor	1.10±0.15	0.51±0.70	0.00±0.04
F110I-MUT-rigor	1.64±0.09	4.49±7.02	0.10±0.08
F110I-WT-con	0.87±0.13	-0.60±0.29	0.15±0.05
F110I-MUT-con	1.04±0.37	0.09±1.48	0.16±0.06

Table 5.
Mean and Standard Deviation of Skewness and Kurtosis of 25 heart muscles expressing R278C mutation

Sample	Skewness±SD	Kurtosis±SD	Peak±SD
R278C-WT-rigor	0.99±0.32	0.19±1.19	0.26±0.12
R278C-MUT-rigor	1.23±0.48	1.66±3.41	0.04±0.09
R278C-WT-con	0.70±0.16	-0.80±0.28	0.13±0.18
R278C-MUT-con	0.86±0.25	-0.33±1.08	0.14±0.14

CHAPTER 4

DISCUSSION

This report demonstrates that the hypertrophic phenotype associated with FHC mutations in TnT is manifested by large difference in the center and width of distributions of orientation of WT vs. MUT cross-bridges. The increase of FWMHs in MUT myofibrils indicates the loss of order of rigor attachment of the cross-bridges. This effect was clearly visible in the velocity plots of all the data (**Fig. 13**). The effect was qualitatively demonstrated in **Figs. 15-17** which showed that. centers and widths of histograms of mutated myofibrils were dramatically larger than that of WT controls. **Table 1** quantified this result.

The PF values clustered around two distinct values of polarization (**Table 2, Fig. 18**). This was not surprising because fluorescence is contributed by cross-bridges which interact with actin carrying both WT and MUT TnT. We note that this effect can only be seen in mesoscopic measurements. Conventional measurements, containing contributions from billions of cross-bridges, offer no hope in detecting two populations,

A different way to demonstrate loss of rigor order in cross-bridges of MUT myofibrils is to calculate skewness (S) and kurtosis (K) of histograms. **Tables 3-5** show that mutation was associated with increase of both S & K in rigor myofibrils. While S & K by themselves do not prove that the disorder of cross-bridges decreased, they do demonstrate that rigor orientations of cross-bridges in mutated muscle is strikingly different from rigor orientations in WT muscle.

The large dispersion of polarization values observed for mutated myofibrils in rigor could be due

either to rotations of the neck region of myosin which do not require hydrolysis of ATP or to the disorder of attachment of myosin to actin carrying mutated TnT. That the observation was made in rigor state does not automatically exclude the possibility that the lever arms rotate. For example, in the model of Coureux, Houdusse and Sweeney, [29] the release of phosphate causes a force-generating conformational change of the bound head. In this low energy state both ADP and actin are bound to myosin head (ADP is bound weakly hence this state is called "weak ADP binding state"). Dissociation of ADP transforms this state to a rigor conformation in which myosin, devoid of hydrolytic products, binds strongly to actin. The global conformation of a cross-bridge in a weak ADP binding state is nearly the same as in rigor, but conformation of LC1 can be completely different. Transition between those states can result in large changes of

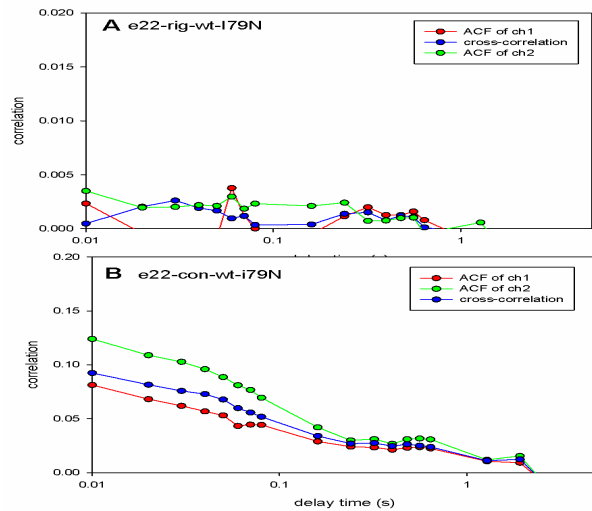


Figure 19A, 19B

orientation of LC1 without hydrolysis of ATP. To test this possibility we measured correlation function in rigor, relaxation and contraction.

Fig. 19A shows that rigor heads do not rotate. Non-zero correlation arises when the fluorescence intensity within the DV changes [26, 30], which in our case arises because transition dipoles of rhodamine change orientation. Conversely, zero correlation arises when the fluorescence intensity within the DV is constant because transition dipoles of rhodamine do not change orientation. **Fig. 19A** indicates that heads in rigor do not move, i.e. it is impossible that disorder arises from motion of lever arm in rigor. In other words, the myosin heads are stationary and disordered. Conversely, **Fig. 19B** shows that during contraction the lever arm rotates.

The large range of polarizations observed in mutated hearts in rigor can, in principle, be translated into range of angles that the transition dipole of rhodamine assumes with respect to the myofibrillar axis. However, such translation has not been attempted here because it is critically dependent on the model of arrangement of cross-bridges. For example, in the model of Tregebar & Mendelson [15] which assumes that the cross-bridges are arranged helically along the long axis of muscle and that polarized fluorescence contains $\alpha\%$ contribution from random immobilized component, the angle is not independent on α , i.e. it can range from 90° to 5° depending on the value of α [15].

In earlier global studies, fluorescent probes were used to study the breadth of orientation distribution of probes bound to RLC of skeletal muscle myosin. Thus Ling et al. [19] and later Hopkins et al. [4] reported that the breadth of distribution of cross-bridges in skeletal muscle was

essentially the same in different physiological states.

Similarly to TnT mutations, 25 experiments on FHC hearts containing A13T mutation in the regulatory light chain revealed a significant increase in the range of polarizations (data not shown). The average skewness of mutated myofibrils in rigor increased by 20% and kurtosis increased by 132% over WT myofibrils in rigor. Thus it is likely that an increase in rigor disorder is a general phenomenon i.e. the stereospecific rigor attachment of force generating myosin cross-bridges is necessary for the normal working of the heart. Any alteration of this important energetic state of the myosin motor could be a triggering factor of cardiomyopathy.

The following four possible artifacts are unlikely to happen:

1. *The fluctuations in orientation are caused by muscle movement, not by cross-bridge rotations. Since rigor muscle does not move, it is different than control.* This is impossible because WT myofibrils were in rigor (i.e. do not move) yet give the small variation in angles (**Fig. 15-17**). Also, it must be remembered that myofibrils were cross-linked. Even when contraction was induced by adding ATP myofibrils do not shorten. Control experiments using skeletal muscle, where we measured sarcomere length as a function of concentration of cross-linker, showed no shortening in confocal microscope when myofibrils were cross-linked with 20 mM EDC.
2. *The differences in dispersion of orientations are caused by cross-linking.* This is impossible because all samples were cross-linked, even those (in rigor) that do not require cross-linking. Besides, we have carried out control experiments using skeletal

muscle where we measured effect of 20 mM EDC on dispersion of polarization and observed no effect.

3. *The effect would be unobservable if the data was fitted by curves different than Gaussian.*

This is unlikely because when we fitted some control skeletal data to Lorentzian and Voigt equations, we observed that they are all very similar to the Gaussian fit.

4. *The effect is not due to the loss of stereospecificity of rigor attachments but is due to an increase in disorganization of actin filaments.* This is unlikely because skewness, kurtosis and center peak positions of histograms are not statistically different for WT and MUT myofibrils in contraction (**Tables 3-5**). Moreover, both WT and MUT myofibrils give the same narrow distribution of orientations in contraction (data not shown).

REFERENCES

1. Geeves, M.A. and K.C. Holmes, *The molecular mechanism of muscle contraction*. Adv Protein Chem., 2005. **71**(24): p. 161-193.
2. Sabido-David, C., S.C. Hopkins, L.D. Saraswat, S. Lowey, Y.E. Goldman, and M. Irving, *Orientation changes of fluorescent probes at five sites on the myosin regulatory light chain during contraction of single skeletal muscle fibres*. J Mol Biol, 1998. **279**(2): p. 387-402.
3. Hopkins, S.C., C. Sabido-David, J.E. Corrie, M. Irving, and Y.E. Goldman, *Fluorescence polarization transients from rhodamine isomers on the myosin regulatory light chain in skeletal muscle fibers*. Biophys J, 1998. **74**(6): p. 3093-110.
4. Hopkins, S.C., C. Sabido-David, U.A. van der Heide, R.E. Ferguson, B.D. Brandmeier, R.E. Dale, J. Kendrick-Jones, J.E. Corrie, D.R. Trentham, M. Irving, and Y.E. Goldman, *Orientation changes of the myosin light chain domain during filament sliding in active and rigor muscle*. J Mol Biol., 2002. **318**(5): p. 1275-91.
5. Miller, T., D. Szczesna, P.R. Housmans, J. Zhao, F. de Freitas, A.V. Gomes, L. Culbreath, J. McCue, Y. Wang, Y. Xu, W.G. Kerrick, and J.D. Potter, *Abnormal contractile function in transgenic mice expressing a familial hypertrophic cardiomyopathy-linked troponin T (I79N) mutation*. J Biol Chem., 2001. **276**(6): p. 3743-55. Epub 2000 Nov 1.
6. Hernandez, O.M., D. Szczesna-Cordary, B.C. Knollmann, T. Miller, M. Bell, J. Zhao, S.G. Sirenko, Z. Diaz, G. Guzman, Y. Xu, Y. Wang, W.G. Kerrick, and J.D. Potter, *F110I and R278C troponin T mutations that cause familial hypertrophic cardiomyopathy affect muscle contraction in transgenic mice and reconstituted human cardiac fibers*. J Biol Chem, 2005. **280**(44): p. 37183-94.
7. Willott, R.H., A.V. Gomes, A.N. Chang, M.S. Parvatiyar, J.R. Pinto, and J.D. Potter, *Mutations in Troponin that cause HCM, DCM AND RCM: what can we learn about thin filament function?* J Mol Cell Cardiol, 2010. **48**(5): p. 882-92.
8. Qian, H., S. Saffarian, and E.L. Elson, *Concentration fluctuations in a mesoscopic oscillating chemical reaction system*. Proc Natl Acad Sci U S A., 2002. **99**(16): p. 10376-81. Epub 2002 Jul 17.
9. Dos Remedios, C.G., R.G. Millikan, and M.F. Morales, *Polarization of tryptophan fluorescence from single striated muscle fibers. A molecular probe of contractile state*. J. Gen. Physiol., 1972. **59**: p. 103-120.
10. Dos Remedios, C.G., R.G. Yount, and M.F. Morales, *Individual states in the cycle of muscle contraction*. Proc Natl Acad Sci U S A, 1972. **69**: p. 2542-2546.
11. Nihei, T., Mendelson, R.A., & Botts, J., *Use of fluorescence polarization to observe changes in attitude of S1 moieties in muscle fibers*. Biophys. J. , 1974. **14** p. 236-242.
12. Tregear, R.T. and R.A. Mendelson, *Polarization from a helix of fluorophores and its relation to that obtained from muscle*. Biophys. J., 1975. **15**: p. 455-467.

13. Morales, M.F., *Calculation of the polarized fluorescence from a labeled muscle fiber.* Proc Nat Acad Sci USA 1984. **81**: p. 145-9.
14. Muthu, P., P. Mettikolla, N. Calander, R. Luchowski, I. Gryczynski, I. Gryczynski, D. Szczesna-Cordary, and J. Borejdo, *Single Molecule Kinetics in the Familial Hypertrophic Cardiomyopathy D166V Mutant Mouse Heart.* Journal of Molecular and Cellular Cardiology, 2009. **48**(6): p. 1264-71.
15. Midde, K., R. Luchowski, H.K. Das, J. Fedorick, V. Dumka, I. Gryczynski, Z. Gryczynski, and J. Borejdo, *Evidence for pre-and post-power stroke of cross-bridges of contracting skeletal myofibrils* Biophys. J., 2011. **in press**.
16. Ling, N., C. Shrimpton, J. Sleep, J. Kendrick-Jones, and M. Irving, *Fluorescent probes of the orientation of myosin regulatory light chains in relaxed, rigor, and contracting muscle.* Biophys. J., 1996. **70**: p. 1836-1846.
17. Herrmann, C., C. Lionne, F. Travers, and T. Barman, *Correlation of ActoS1, myofibrillar, and muscle fiber ATPases.* Biochemistry, 1994. **33**(14): p. 4148-54.
18. Tsaturyan, A.K., S.Y. Bershitsky, R. Burns, and M.A. Ferenczi, *Structural changes in the actin-myosin cross-bridges associated with force generation induced by temperature jump in permeabilized frog muscle fibers.* Biophys J, 1999. **77**(1): p. 354-72.
19. Borejdo, J., P. Muthu, J. Talent, I. Akopova, and T.P. Burghardt, *Rotation of Actin Monomers during Isometric Contraction of Skeletal Muscle.* J. Biomed. Optics, 2007. **12**(1): p. 014013.
20. Baudenbacher, F., T. Schober, J.R. Pinto, V.Y. Sidorov, F. Hilliard, R.J. Solaro, J.D. Potter, and B.C. Knollmann, *Myofilament Ca²⁺ sensitization causes susceptibility to cardiac arrhythmia in mice.* J Clin Invest, 2008. **118**(12): p. 3893-903.
21. Szczesna, D. and S.S. Lehrer, *The binding of fluorescent phallotoxins to actin in myofibrils.* J Muscle Res Cell Motil, 1993. **14**(6): p. 594-7.
22. Ao, X. and S.S. Lehrer, *Phalloidin unzips nebulin from thin filaments in skeletal myofibrils.* J Cell Sci, 1995. **108**(Pt 11): p. 3397-403.
23. Magde, D., E.L. Elson, and W.W. Webb, *Fluorescence correlation spectroscopy. II. An experimental realization.* Biopolymers, 1974. **13**(1): p. 29-61.
24. Elson, E.L., *Introduction to FCS.* Short Course on Cellular and Molecular Fluorescence, ed. Z. Gryczynski. Vol. 2. 2007, Fort Worth: UNT. 1-10.
25. Borejdo, J., D. Szczesna-Cordary, P. Muthu, and N. Calander, *Familial Hypertrophic Cardiomyopathy Can Be Characterized by a Specific Pattern of Orientation Fluctuations of Actin Molecules.* Biochemistry, 2010. **49**: p. 5269-5277.
26. Elson, E.L. and D. Magde, *Fluorescence Correlation Spectroscopy: Coceptual Basis and Theory.* Biopolymers, 1974. **13**: p. 1-28.
27. Coureux, P.D., H.L. Sweeney, and A. Houdusse, *Three myosin V structures delineate essential features of chemo-mechanical transduction.* Embo J, 2004. **23**(23): p. 4527-37.